Anti-sclerostin antibodies and abaloparatide have additive effects when used as a countermeasure against disuse osteopenia in female rats

Brent, Mikkel Bo; Brüel, Annemarie; Thomsen, Jesper Skovhus

Published in:
Bone

DOI (link to publication from Publisher):
10.1016/j.bone.2022.116417

Publication date:
2022

Document Version
Publisher's PDF, also known as Version of record

Bone 160 (2022) 116417

Contents lists available at ScienceDirect

Bone

journal homepage: www.elsevier.com/locate/bone

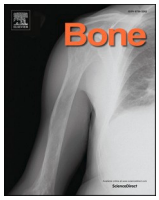

Full Length Article

Anti-sclerostin antibodies and abaloparatide have additive effects when used as a countermeasure against disuse osteopenia in female rats

Mikkel Bo Brent [a,b,*], Annemarie Brüel [a,1], Jesper Skovhus Thomsen [a,1]

[a] Department of Biomedicine, Aarhus University, Aarhus, Denmark
[b] Department of Orthopedic Surgery, Aalborg University Hospital, Aalborg, Denmark

ARTICLE INFO

Keywords:
DXA
Osteoporosis
Bone loss
Abaloparatide
Romosozumab
Scl-Ab

ABSTRACT

Prolonged disuse and substantial mechanical unloading are particularly damaging to skeletal integrity. Preclinical studies in rodents and clinical studies have highlighted the need for potent bone anabolic drugs to counteract disuse-induced osteopenia. The aim of present study was to compare the efficacy of romosozumab (Scl-Ab) and abaloparatide (ABL), alone or in combination, to prevent botulinum toxin (BTX) induced bone loss in a rat model. Eighty female Wistar rats were divided into the following six groups: 1. Baseline ($n = 12$); 2. Control (Ctrl) ($n = 12$); 3. BTX ($n = 12$); 4. BTX + Scl-Ab ($n = 16$); 5. BTX + ABL ($n = 12$); and 6. BTX + Scl-Ab + ABL ($n = 16$). Disuse was achieved by injecting 4 IU BTX into the hind limb musculature at study start. Scl-Ab (25 mg/kg) was injected s.c. twice weekly, while ABL (80 μg/kg) was injected s.c. five days a week for four weeks. Hind limb disuse dramatically decreased muscle mass and skeletal integrity and deteriorated the cortical morphology and trabecular microstructure. Treatment with Scl-Ab alone prevented most of the adverse cortical and trabecular effects of disuse, while ABL monotherapy mainly attenuated the disuse-induced loss of femoral areal bone mineral density (aBMD). Moreover, the combination of Scl-Ab and ABL not only counteracted most of the negative skeletal effects of unloading, but also increased aBMD (+10% and +20%), epiphyseal trabecular bone volume fraction (BV/TV) (+25% and +73%), and metaphyseal bone strength (+18% and +30%) significantly above that of Scl-Ab or ABL monotherapy, respectively. The potent and additive osteoanabolic effect of Scl-Ab and ABL, when given in combination, is highly intriguing and underlines that an osteoanabolic bone gain can be maximized by utilizing two pharmaceuticals targeting different cellular signaling pathways. From a clinical perspective, a combination treatment may be warranted in patients where the osteoanabolic effect of either monotherapy is not sufficient, or if a dose-reduction is required due to adverse effects.

1. Introduction

Osteoporosis is a skeletal disease characterized by reduced bone mineral density and susceptibility to fragility fractures [1]. The disease manifests as the consequence of increased bone resorption relative to bone formation, thus resulting in a net bone loss. Multiple non-modifiable and potentially modifiable risk factors are associated with osteoporosis [2,3]. Of potentially modifiable risk factors for osteoporosis, skeletal loading is particularly important. The earliest studies of disuse in paralyzed dogs and subsequent clinical studies in paralyzed patients emerged around the beginning of the last century [4–6]. These early landmark studies highlighted the importance of mechanical loading for maintaining skeletal integrity and marked the beginning of meticulous research efforts into the nature of disuse and the pharmaceutical countermeasures against it.

Our understanding of the underlying cellular and molecular mechanisms responsible for disuse-induced bone loss has been propelled by the discovery of the Wnt signaling pathway and its role in bone. The Wnt signaling pathway and its relevance for bone homeostasis is very complex and has been described in detail elsewhere [7,8]. In brief, when Wnt ligands interact with the dual receptor complex involving the Frizzled (FZD) receptor and low-density lipoprotein receptor-related protein (LRP)-5 or -6 expressed on osteoblasts, an intracellular signaling cascade is initiated, resulting in activation and transcription of target genes important for osteoblast differentiation and proliferation as well as for bone formation. Wnt signaling can be antagonized by

* Corresponding author at: Department of Biomedicine, Health, Aarhus University, Wilhelm Meyers Allé 3, DK-8000 Aarhus C, Denmark.
E-mail address: mbb@biomed.au.dk (M.B. Brent).
[1] AB and JST are joint senior authors

https://doi.org/10.1016/j.bone.2022.116417
Received 24 February 2022; Received in revised form 1 April 2022; Accepted 4 April 2022
Available online 7 April 2022

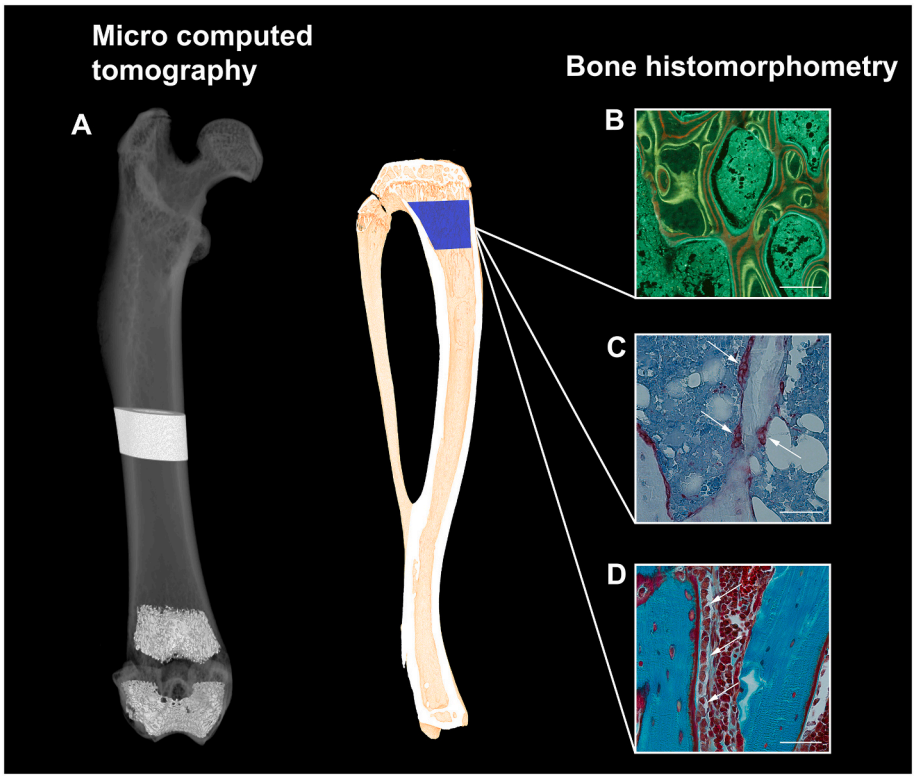

Fig. 1. A) Illustration of a rat femur with the volumes of interest (VOIs) at the femoral mid-diaphysis and distal metaphysis and epiphysis used for micro computed tomography analysis. B–D) Bone histomorphometry at the tibial proximal metaphysis. B) Dynamic bone histomorphometry to assess bone remodeling. Bar = 150 μm. C) Section stained for tartrate-resistant acid phosphatase (TRAP) and counterstained with aniline blue to detect osteoclasts (white arrows). Bar = 50 μm. D) Masson-Goldner trichrome-stained section for osteoblasts (white arrows) and osteoid. Bar = 50 μm. (For interpretation of the references to colour in this figure legend, the reader is referred to the web version of this article.)

Table 1
The number of animals allocated to each group, body weight (BW), and wet weight and whole muscle cross-sectional area of the right rectus femoris muscle, and femoral length from rats subjected to hind limb disuse and treated with romosozumab (Scl-Ab) or abaloparatide (ABL) for four weeks. Data are presented as mean ± SD.

	Baseline	Ctrl	BTX	BTX + Scl-Ab	BTX + ABL	BTX + Scl-Ab + ABL
Animals (*n*)	12	12	12	16	12	16
Start BW (g)	250 ± 9.37	248 ± 9.35	249 ± 9.41	250 ± 6.39	247 ± 8.02	247 ± 6.87
Final BW (g)	250 ± 9.37	270 ± 11.4	247[a] ± 13.9	249[a] ± 8.68	244[a] ± 11.9	250[a] ± 7.74
Rectus femoris muscle						
Wet weight (mg)	680 ± 49.4	790 ± 65.5	240[a] ± 27.7	231[a] ± 22.3	223[a] ± 22.1	232[a] ± 39.9
CSA (mm^2)	51.3 ± 5.70	52.4 ± 5.96	20.4[a] ± 3.78	21.4[a] ± 4.61	18.8[a] ± 2.45	19.5[a] ± 4.05
Femoral bone						
Length (mm)	32.5 ± 0.71	33.9 ± 0.54	33.9 ± 0.73	34.0 ± 0.67	34.2 ± 0.68	34.2 ± 0.41

[a] $p < 0.05$ vs. Ctrl.

inhibitors such as sclerostin secreted from osteocytes, which prevents the formation of the Wnt-FZD-LRP5 complex by competitive binding to LRP5 and internalization of the LRP5/6 co-receptor [9].

Mounting evidence from preclinical and clinical studies has demonstrated that unloading and disuse results in heavy upregulation of *SOST* and increased serum sclerostin levels [10–12]. In contrast, sclerostin levels are dramatically reduced by mechanical loading and weight bearing [13]. Thus, anti-sclerostin antibodies are a potential pharmaceutical countermeasure against disuse-induced bone loss.

Romosozumab is a humanized monoclonal antibody targeting sclerostin that has demonstrated promising efficacy to attenuate disuse-induced bone loss in rodent studies [14–16]. Although romosozumab is effective as monotherapy, a substantially greater bone formation response may be achieved by combining its effect with that of another potent bone anabolic agent such as teriparatide or abaloparatide. Both intermittent teriparatide and abaloparatide are potent stimulators of net bone formation and act through the parathyroid hormone 1 receptor (PTH1R) expressed on osteoblasts [17,18]. However, their osteoanabolic effect is blunted in *SOST* overexpressing mice [19] and in hind limb unloaded rats [20,21], thus suggesting that their bone-forming capacity could be enhanced by concomitant treatment with anti-sclerostin antibodies.

We hypothesize that the combination of pharmaceutical countermeasures utilizing two different cellular signaling pathways, anti-sclerostin antibodies and PTH1R-stimulation, results in substantially increased bone formation compared with either treatment alone. From a clinical perspective, an additive skeletal effect of anti-sclerostin antibodies and abaloparatide is particularly intriguing, since it may justify a dose reduction to benefit patients experiencing dose-dependent adverse effects or reduce treatment costs.

The present study aimed to investigate whether romosozumab and abaloparatide in combination elicit an additive osteoanabolic effect that is superior to either treatment alone in the prevention of disuse-induced bone loss originating from injections with botulinum toxin (BTX) in rats.

2. Material and methods

2.1. Animals and study design

Eighty female 12–13-week-old Wistar rats were purchased from Janvier Labs (Le Genest-Saint-Isle, France). Upon arrival, the rats were allowed one week of acclimatizing before study start and were then stratified by body weight into six groups: 1. Baseline ($n = 12$); 2. Control

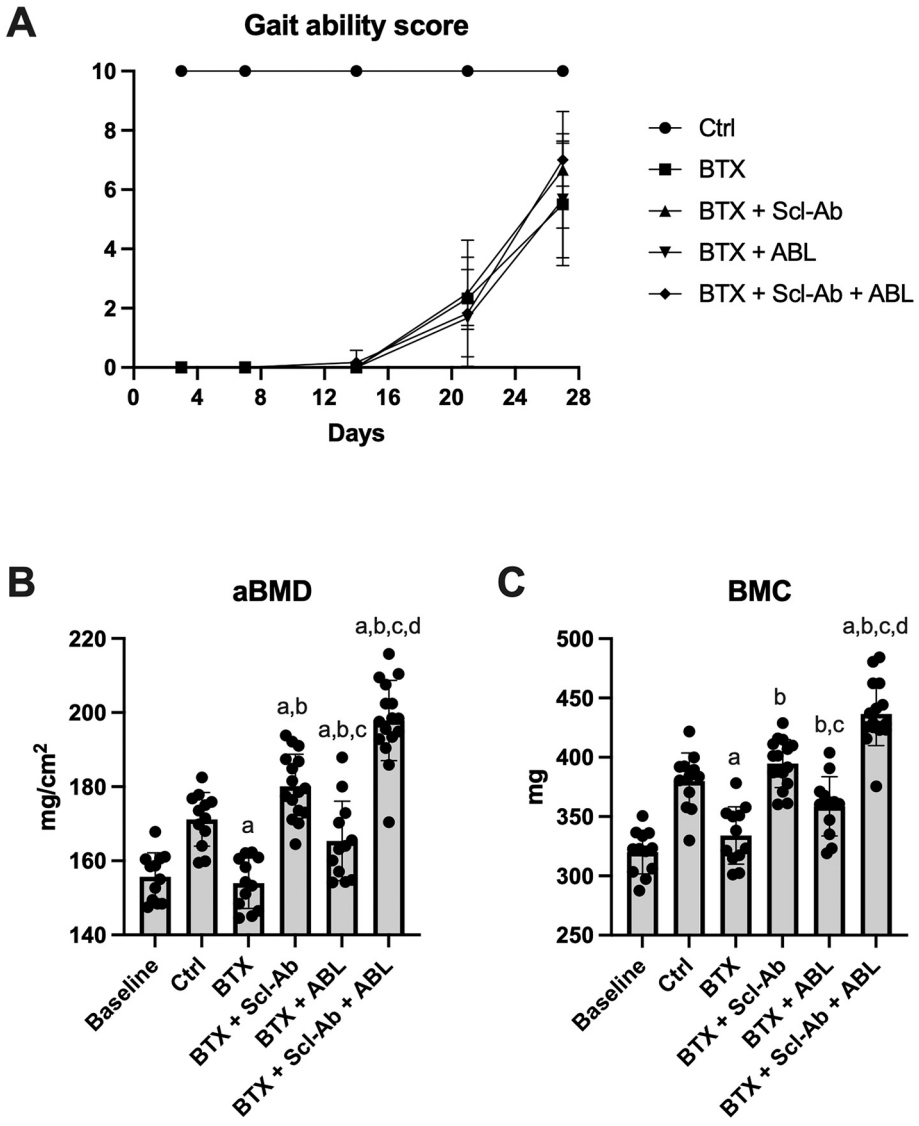

Fig. 2. A) Gait ability score, B) areal bone mineral density (aBMD), and C) bone mineral content (BMC) from rats subjected to hind limb disuse and treated with romosozumab (Scl-Ab) or abaloparatide (ABL) alone or in combination for four weeks. The gait ability decreased dramatically in all botulinum toxin (BTX) injected rats and started to recover after 14 days. Data are presented as mean ± SD. [a]: $p < 0.05$ vs. Ctrl. [b]: $p < 0.05$ vs. BTX. [c]: $p < 0.05$ vs. BTX + Scl-Ab. [d]: $p < 0.05$ vs. BTX + ABL.

(Ctrl) ($n = 12$), 3. BTX ($n = 12$), 4. BTX + romosozumab (Scl-Ab) ($n = 16$), 5. BTX + abaloparatide (ABL) ($n = 12$), and BTX + Scl-Ab + ABL ($n = 16$). At study start, the rats were 13–14 weeks old with a mean body weight of 237 ± 11.1 g. Chemical nerve denervation by BTX was used to induce disuse as proposed by Chappard et al. [22]. Animals assigned to the BTX-groups were intramuscularly injected with 4 IU of BTX type A (Botox, Allergan, Dublin, Ireland) distributed into their right quadriceps, hamstring, and calf muscles to induce disuse, as previously described in detail [23]. Throughout the study, all rats had unrestricted access to pelleted chow (1324 maintenance diet for rats and mice; Altromin, Lage, Germany) and tap water and were housed groupwise ($n = 4$/cage) at 20 °C with a 12:12 h light/dark cycle.

The anti-sclerostin antibody romosozumab was purchased from Amgen (Amgen Inc., Thousand Oaks, CA, USA) and injected s.c. twice weekly (25 mg/kg) [14]. Because romosozumab is a humanized monoclonal antibody, and therefore immunogenic to rats, the Scl-Ab groups were powered to allow the exclusion of rats that developed anti-drug antibodies (ADA) and an attenuated pharmacological response. The parathyroid hormone-related protein (PTHrP) analog abaloparatide was purchased from Bachem (H-8334, Bachem AG, Bubendorf, Switzerland) and injected s.c. five times a week (80 μg/kg) [24]. Treatment with Scl-Ab and abaloparatide commenced on the first day of the study, where disuse was induced by BTX injections, and continued until sacrifice.

Tetracycline double labels (20 mg/kg, T3383, Sigma-Aldrich, St. Louis, MO, USA) and alizarin double labels (20 mg/kg, A3882, Sigma-Aldrich, St. Louis, MO, USA) were injected to assess bone remodeling in week 0–1 and week 2–3, respectively.

To assess the physiological effect of hind limb injections with BTX, six rats from each group were evaluated using the gait ability score developed by Warner et al. [25] The score ranges from 0 (completely disabled) to 2 (normal) and assesses five different items of motor function. In brief, the gait ability score includes the following assessments: Hindlimb abduction during tail suspension, toe extension during sitting, use of right leg during leveled walking, use of right leg during two-legged stance, and use of right leg during climbing resulting in a total score from 0 to 10 [23].

After four weeks of disuse and treatment, the animals were sacrificed under anesthesia with 3% isoflurane (IsoFlo Vet, Orion Pharma Animal Health, Nivå, Denmark).

Animal handling and injections were conducted unblinded to group allocation. Investigators were blinded for group allocation for the assessment of bone remodeling indices by dynamic bone histomorphometry and quantification of bone cells, whereas the remaining analyses were performed unblinded. However, all laboratory procedures were conducted across group allocations in order to minimize any

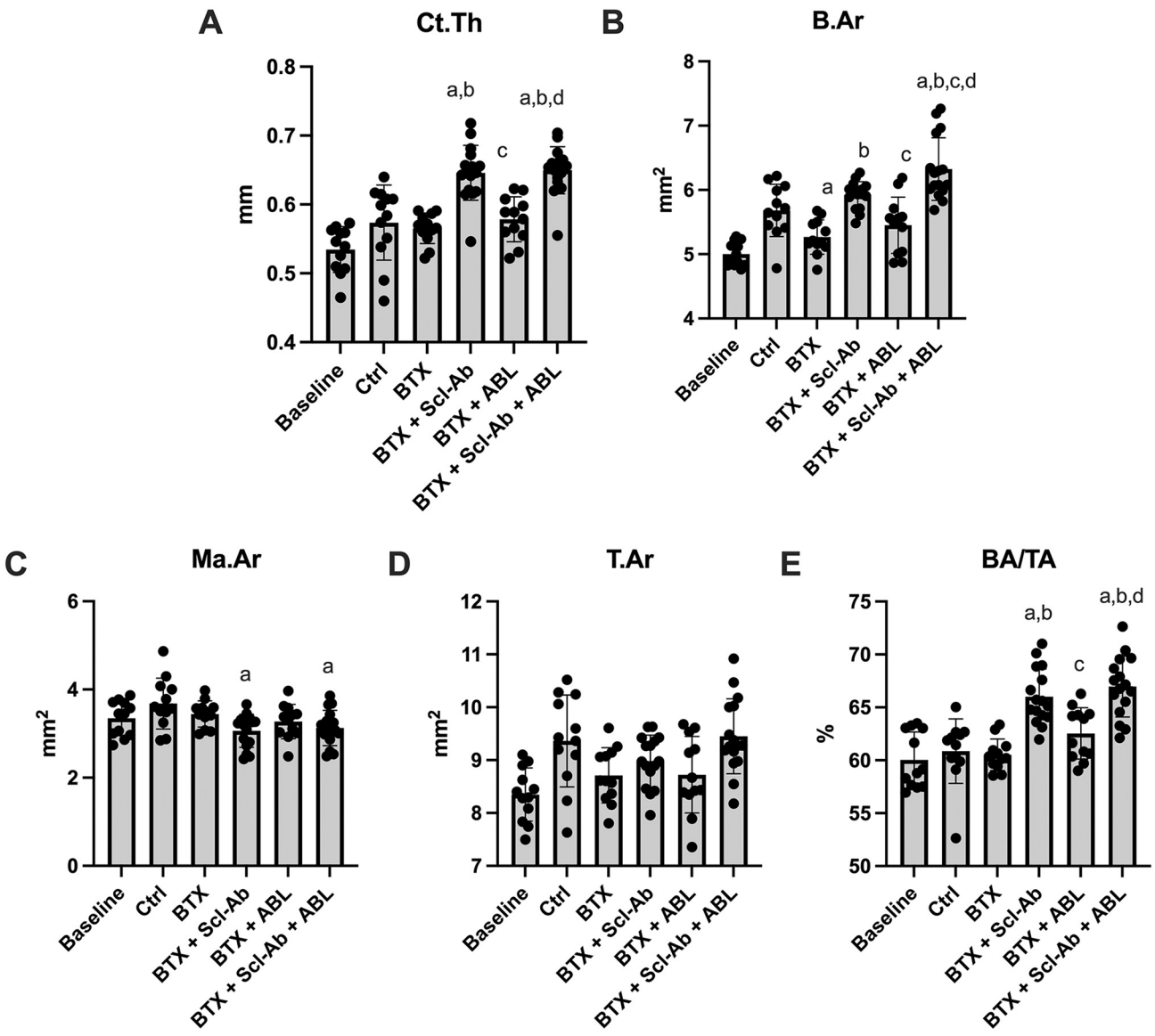

Fig. 3. Femoral mid-diaphyseal cortical morphology of rats subjected to hind limb disuse and treated with romosozumab (Scl-Ab) or abaloparatide (ABL) alone or in combination for four weeks. A) Cortical thickness (Ct.Th). B) Bone area (B.Ar). C) Marrow area (Ma.Ar). D) Tissue area (T.Ar). E) Bone area/tissue area (BA/TA). Data are presented as mean ± SD. [a]: $p < 0.05$ vs. Ctrl. [b]: $p < 0.05$ vs. BTX. [c]: $p < 0.05$ vs. BTX + Scl-Ab. [d]: $p < 0.05$ vs. BTX + ABL.

impact of experimental bias.

All animal procedures were approved by the Danish Animal Inspectorate (2018-15-0201-01436). The animal welfare was assessed daily by veterinarians, animal caretakers, or study investigators.

2.2. Tissue extraction

Immediately after sacrifice, the right hind limb was removed, and the rectus femoris muscle, femur, and tibia were carefully isolated. The wet weight of the rectus femoris muscle was determined using a digital scale (Mettler AT250, Columbus, OH, USA) before being immersion-fixed in 0.1 M sodium phosphate-buffered formaldehyde (4% formaldehyde, pH 7.0).

The right femoral bone length was measured using a digital caliper and stored in Ringer's solution at −20 °C. The right tibia was immersion-fixed in 0.1 M sodium phosphate-buffered formaldehyde (4% formaldehyde, pH 7.0) for 48 h and then stored in 70% ethanol.

2.3. Rectus femoris muscle

The right rectus femoris muscle was halved at the midpoint and placed on a flat-bed image scanner (Perfection 3200 Photo; Seiko Epson, Nagano, Japan) to determine the whole muscle cross-sectional area (CSA) as previously described [23]. In brief, the scanning was conducted at 300 dots per inch (DPI), images were analyzed in Adobe Photoshop 2020 (San Jose, California, USA) using the inbuilt ruler and measure tools, and the muscles CSA were delineated using the Lasso Tool.

2.4. Dual-energy X-ray absorptiometry (DXA)

Areal bone mineral density (aBMD) and bone mineral content (BMC) of the entire femur were determined by DXA (pDEXA Sabre XL; Norland Stratec, Pforzheim, Germany) at a resolution of 0.5 mm × 0.5 mm and a scan speed of 10.0 mm/s.

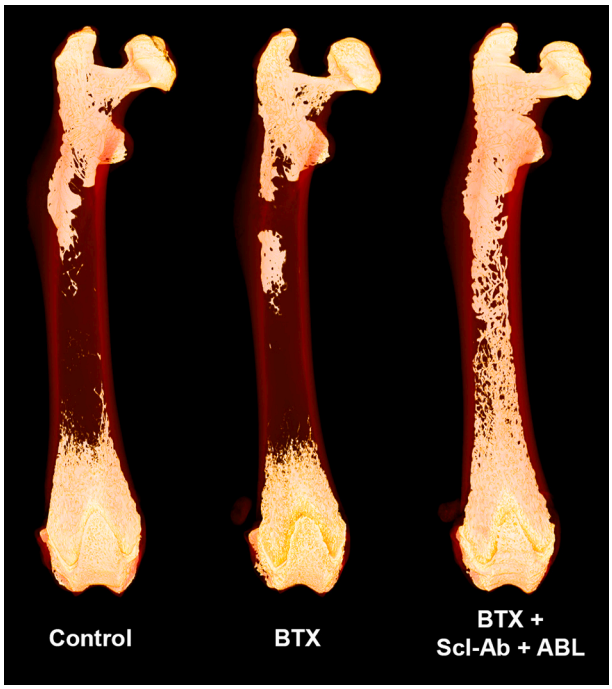

Fig. 4. 3D reconstructions of μCT data of the entire right femur from one rat injected with saline (Control); botulinum toxin (BTX); or BTX, romosozumab (Scl-Ab), and abaloparatide (ABL) for four weeks. Cortical bone is presented in semi-transparent red, allowing the appearance of the underlying trabecular bone to be visualized. The amount of trabecular bone in the marrow cavity was high in a few of the animals treated with the combination of Scl-Ab and ABL. However, it should be emphasized the majority of the rats treated with Scl-Ab did not develop such pronounced trabecular bone at the femoral mid-diaphysis. μCT voxel size: 10 μm. (For interpretation of the references to colour in this figure legend, the reader is referred to the web version of this article.)

2.5. Micro computed tomography (μCT)

The femoral bone morphology and trabecular microstructure were assessed using a desktop μCT scanner (Scanco μCT 35, Scanco Medical AG, Wangen-Brüttisellen, Switzerland). The femoral mid-diaphysis, distal femoral metaphysis, and distal femoral epiphysis were scanned using 1000 projections/180°, an isotropic voxel size of 10 μm, an X-ray tube voltage of 70 kVp, a current of 114 μA, and an integration time of 800 ms. Beam hardening effects were reduced using a 0.5 mm aluminum filter.

The femoral mid-diaphysis was analyzed using two 2320-μm-high volumes of interest (VOIs) centered on the femoral mid-point. One was demarked at the periosteal surface and was used to determine cortical morphology. The other was demarked at the endocortical surface and was used to quantify the amount of trabecular bone in the mid-diaphyseal marrow cavity (Fig. 1).

The trabecular bone at the distal femoral epiphysis was analyzed using an approximately 1500-μm-high VOI containing trabecular bone only. The epiphyseal VOI started where the lateral and medial condyle fused to one coherent structure and ended where the growth plate first appeared. The distal femoral metaphysis was analyzed using a 2200-μm-high VOI starting 1500 μm above the most distal part of the growth plate to exclude primary spongiosa (Fig. 1). All 3D data were low-pass filtered using a Gaussian filter ($\sigma = 0.8$ and support = 1) and segmented with a fixed global threshold of 520 mg HA/cm^3.

The μCT-based assessment of the bone microstructure was performed in accordance with the current guidelines [26].

2.6. Mechanical testing

Bone strength of the femoral mid-diaphysis, femoral neck, and distal femoral metaphysis was determined using a materials-testing machine (5566; Instron, High Wycombe, UK) as previously described in detail [27]. In brief, the 3-point bending test of the femoral mid-diaphysis was conducted by placing the bone on two supporting bars and vertical load was applied using a rounded bar until a complete fracture materialized. Then the proximal part of the femur was placed in a custom-made fixation device to expose the femoral neck for mechanical testing. The vertebral body of L4 was compression tested after vertebral discs and processi were carefully removed. For all the mechanical tests, vertical load was applied with a constant deflection rate of 2 mm/min. Bone strength was considered as the maximum force achieved at any point during mechanical testing and was determined from the load-displacement data.

2.7. Bone specimens and microscopy

A 200-μm-thick cross-sectional slice of the right femoral mid-diaphysis was sawed (EXAKT Apparatebau, Norderstedt, Germany),

Table 2
Femoral trabecular microstructural parameters from rats subjected to hind limb disuse and treated with romosozumab (Scl-Ab) or abaloparatide (ABL) for four weeks. Bone volume/tissue volume (BV/TV), tissue mineral density (TMD), volumetric bone mineral density (vBMD), connectivity density (CD), and structure model index (SMI). Data are presented as mean ± SD.

	Baseline	Ctrl	BTX	BTX + Scl-Ab	BTX + ABL	BTX + Scl-Ab + ABL
Mid-diaphyseal marrow cavity						
BV/TV (%)	1.17 ± 1.25	1.42 ± 1.57	0.75 ± 0.73	0.68 ± 1.14	1.18 ± 1.61	2.39 ± 3.47
Epiphysis						
TMD (mg/cm^3)	869 ± 8.47	887 ± 10.6	876 ± 8.27	890[a,b] ± 10.7	881[c] ± 7.89	907[a,b,d] ± 14.4
vBMD (mg/cm^3)	412 ± 27.3	443 ± 30.8	372[a] ± 26.1	550[a,b] ± 63.1	420[b,c] ± 40.8	654[a,b,c,d] ± 56.0
CD (mm^{-3})	117 ± 18.8	97.5 ± 10.3	110 ± 13.2	73.4[a,b] ± 14.6	101[c] ± 16.1	89.6[b] ± 11.5
SMI	−0.44 ± 0.18	−0.69 ± 0.29	−0.07 ± 0.22	−1.85[b] ± 0.91	−0.45 ± 0.37[c]	−4.74[a,b,d] ± 1.82
Metaphysis						
TMD (mg/cm^3)	877 ± 13.7	901 ± 12.7	899 ± 17.2	890 ± 19.0	884 ± 18.5	897 ± 18.9
vBMD (mg/cm^3)	386 ± 82.3	433 ± 57.8	395 ± 79.2	428 ± 94.6	401 ± 84.5	578[a,b,c,d] ± 87.3
CD (mm^{-3})	213 ± 38.5	230 ± 38.5	268 ± 64.1	98.2[a,b] ± 16.6	140[c] ± 21.2	109[a,b] ± 16.0
SMI	0.19 ± 1.00	−0.19 ± 0.69	0.43 ± 1.01	0.66 ± 0.93	0.64 ± 0.91	−1.73[b,c,d] ± 1.77

[a] $p < 0.05$ vs. Ctrl.
[b] $p < 0.05$ vs. BTX.
[c] $p < 0.05$ vs. BTX + Scl-Ab.
[d] $p < 0.05$ vs. BTX + ABL.

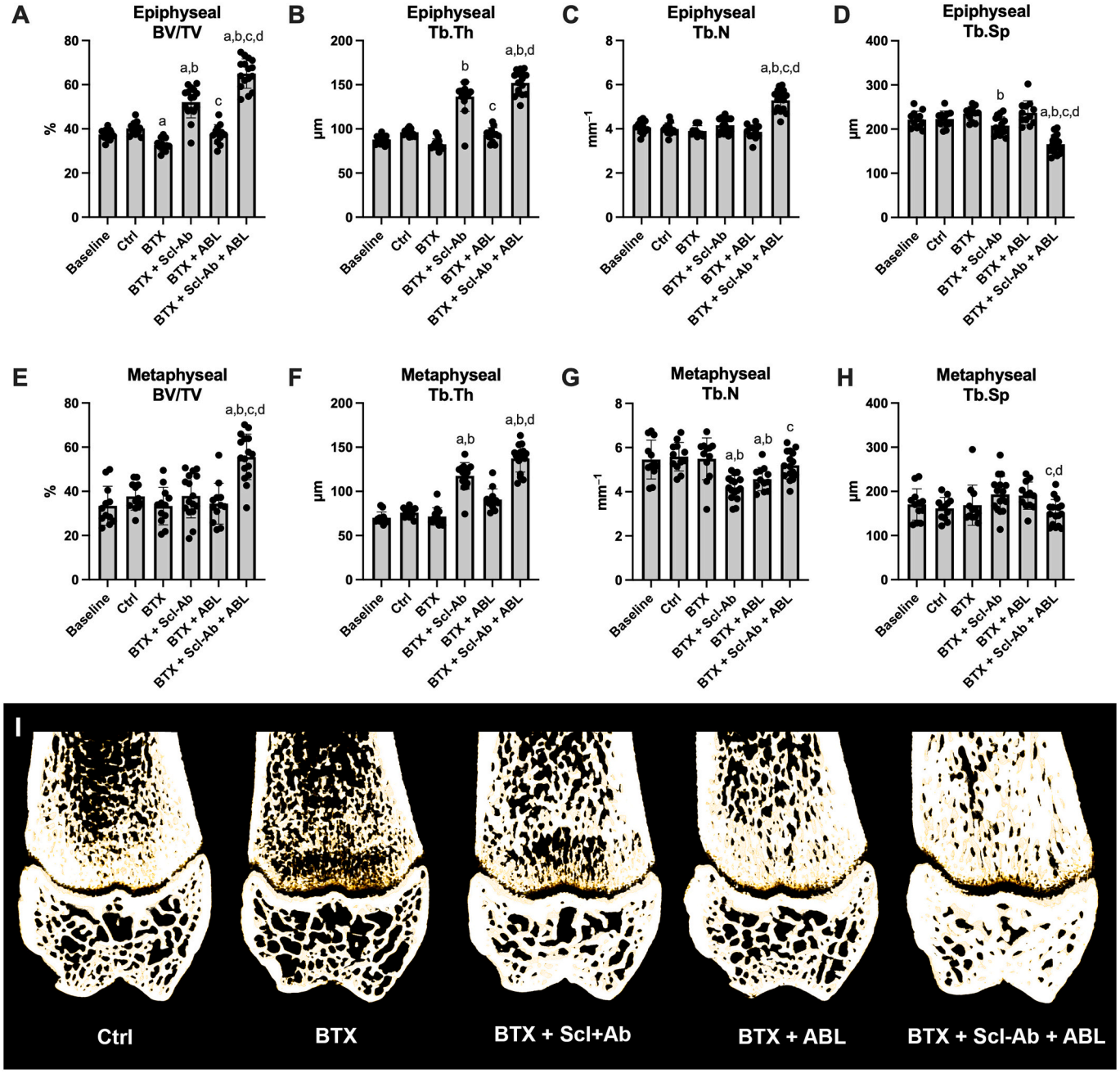

Fig. 5. Trabecular microstructure at the (A–D) femoral distal epiphysis and (E–H) metaphysis of rats subjected to hind limb disuse and treated with romosozumab (Scl-Ab) or abaloparatide (ABL) alone or in combination for four weeks. I) Representative 3D reconstructions of the distal femoral metaphysis and epiphysis (100 µm thick slices). Bone volume/tissue volume (BV/TV), trabecular thickness (Tb.Th), trabecular number (Tb.N), and trabecular spacing (Tb.Sp). Data are presented as mean ± SD. [a]: $p < 0.05$ vs. Ctrl. [b]: $p < 0.05$ vs. BTX. [c]: $p < 0.05$ vs. BTX + Scl-Ab. [d]: $p < 0.05$ vs. BTX + ABL.

mounted with Pertex on a glass slide, and used for dynamic bone histomorphometry. The proximal tibia was either embedded undecalcified in methyl methacrylate (MMA) or decalcified using formic acid and embedded in paraffin. The undecalcified samples were cut into 7-µm-thick frontal sections and left unstained and used for dynamic bone histomorphometry, stained for tartrate-resistant acid phosphatase (TRAP) and counterstained with aniline blue to detect osteoclasts, or Masson-Goldner trichrome-stained for osteoblast and osteoid identification (Fig. 1).

Light and fluorescence microscopy were conducted using a Nikon Eclipse i80 upright microscope (Nikon Solutions, Tokyo, Japan), able to project live images to a computer. The stereological software Visiopharm (v. 2020.09, Visiopharm, Hørsholm, Denmark) was used to quantify fluorochrome labels and bone cells at a final magnification of ×1190. Dynamic bone histomorphometry and bone cell quantifications were conducted in accordance with the guiding principles of the ASBMR Histomorphometry Nomenclature Committee [28].

2.8. Dynamic bone histomorphometry

Dynamic bone histomorphometry was used to assess bone remodeling at week 0–1 and week 2–3. At the femoral mid-diaphysis, a stellar grid with 24-radiating arms was used to quantify the amount of fluorochrome labels at the periosteal and endocortical surfaces. The distance between two consecutive tetracycline or two alizarin labels was measured at the mid-point between two labels. At the proximal tibial

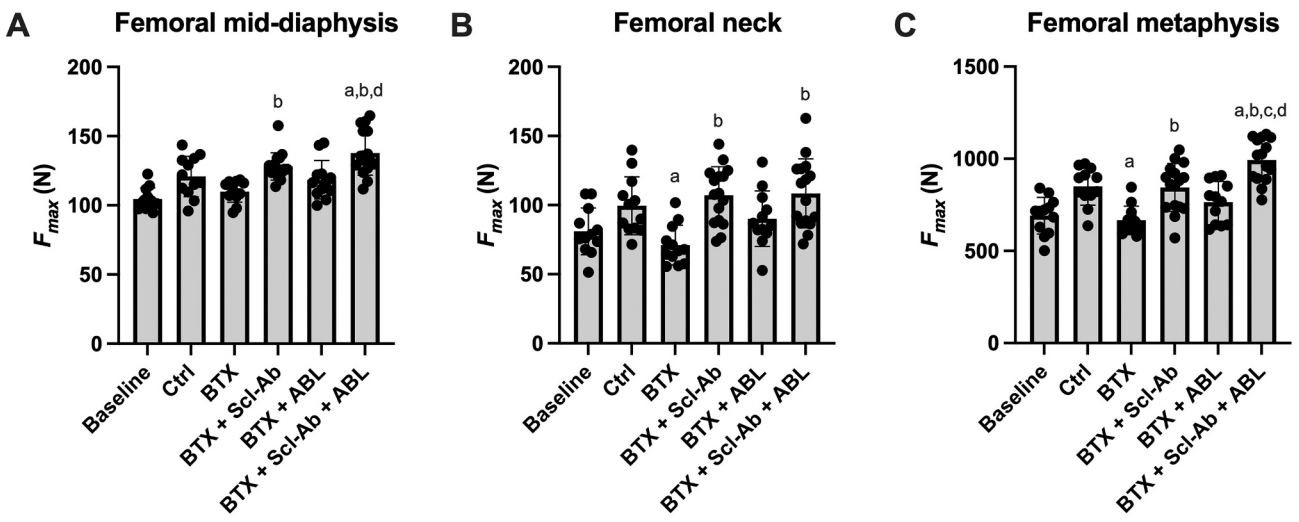

Fig. 6. Bone fracture strength of the (A) femoral mid-diaphysis, (B) femoral neck, and (C) distal femoral metaphysis of rats subjected to hind limb disuse and treated with romosozumab (Scl-Ab) or abaloparatide (ABL) alone or in combination for four weeks. Data are presented as mean ± SD. [a]: $p < 0.05$ vs. Ctrl. [b]: $p < 0.05$ vs. BTX. [c]: $p < 0.05$ vs. BTX + Scl-Ab. [d]: $p < 0.05$ vs. BTX + ABL.

metaphysis, trabecular fluorochrome labels were quantified using a 3000-μm-high region of interest (ROI) placed 1500 μm below the growth plate, excluding primary spongiosa and cortical bone. The fields of view were sampled with a randomly orientated line grid superimposed on the fields of view and covered at least 40% of the ROI.

Dynamic bone histomorphometry was used to estimate mineralizing surface, mineral apposition rate, and bone formation rate. Mineralizing surface was calculated as the number of intersections with double labels plus half the number of intersections with single labels divided by the total number of intersections with an intact bone surface. Mineral apposition rate was calculated as the average distance between double labels divided by the inter-labeling period of seven days. Bone formation rate was calculated as mineralizing surface × mineral apposition [28]. If double labels were absent, then an imputed value of zero was used for mineral apposition.

2.9. Quantification of osteoclasts, osteoid, and osteoblasts

The sections stained for TRAP were used to quantify the amount of osteoclast-covered bone surface. Osteoclasts were defined as TRAP-positive multinucleated cells residing on an intact bone surface. The Masson-Goldner trichrome-stained sections were used to quantify the amount of osteoid and osteoblast-covered surfaces. Bone cells and osteoid were quantified using a 3000-μm-high ROI placed 1500 μm below the growth plate, and the fields of view were sampled with a randomly orientated line grid superimposed on the fields of view that covered at least 40% of the ROI.

2.10. Statistical analysis

Differences between means of the groups were assessed using a one-way analysis of variance (ANOVA) followed by a post-hoc Holm-Sidak test, if the data approximately followed a normal distribution. Otherwise, a non-parametric one-way ANOVA on ranks followed by a post-hoc Dunn's test was used. Equality of variance was assessed using the Brown-Forsythe test. The one-way ANOVA included the groups Ctrl, BTX, BTX + Scl-Ab, BTX + ABL, and BTX + Scl-Ab + ABL. Data are presented as mean ± SD, and results were considered statistically significant if the p-value was less than 0.05. The statistical analyses were performed in GraphPad Prism 9.1.1 (Systat Software, Chicago, IL, USA).

An a priori sample size calculation (power = 0.8) showed that it is possible to demonstrate a difference of 12% in mechanical strength of the femoral mid-diaphysis between groups with 12 animals in each group [29]. Although the two groups treated with Scl-Ab were over-powered to allow the exclusion of animals developing ADA or attenuated pharmacological response, we included all animals in the statistical analyses to give the most accurate representation of its osteoanabolic effect in rats [30]. Moreover, up to 18% of post-menopausal women in the phase 2 and 3 studies developed ADA after their first injection with Scl-Ab [31]. The inclusion of all animals treated with Scl-Ab despite ADA status may therefore more closely resemble the use of Scl-Ab in a clinical setting.

3. Results

3.1. Body weight and gait ability

After four weeks of disuse, the body weight of BTX-injected rats was significantly lower (−8%, $p < 0.001$) than that of Ctrl rats (Table 1). The BTX-injections resulted in a pervasive and rapidly developing muscle paralysis that completely disabled normal hind limb locomotion. However, the gait ability improved after two weeks, although the normal motor function was not restored when the study ended after four weeks (Fig. 2).

3.2. Muscles mass and cross-sectional area

All BTX-injected rats had significantly lower rectus femoris muscle mass (−71%, $p < 0.001$) and whole muscle CSA (−62%, $p < 0.001$) than the rats in the Ctrl group, underlining the detrimental effects of disuse on muscle tissue. Treatment with Scl-Ab and ABL alone, or in combination, did not affect muscle mass or CSA compared with non-treated disuse rats (Table 1).

3.3. DXA

Compared with normal ambulating rats, disuse significantly reduced femoral aBMD (−10%, $p < 0.001$) and BMC (−12%, $p < 0.001$). Treatment with Scl-Ab alone and in combination with ABL not only prevented the disuse-induced loss of aBMD and BMC but significantly increased aBMD (+17%, $p = 0.025$ and 29%, $p < 0.001$) above that of Ctrl rats, respectively. Interestingly, the combination of Scl-Ab and ABL significantly increased aBMD and BMC (+10%, $p < 0.001$ and +20%, $p < 0.001$) above that of treatment with Scl-Ab and ABL alone,

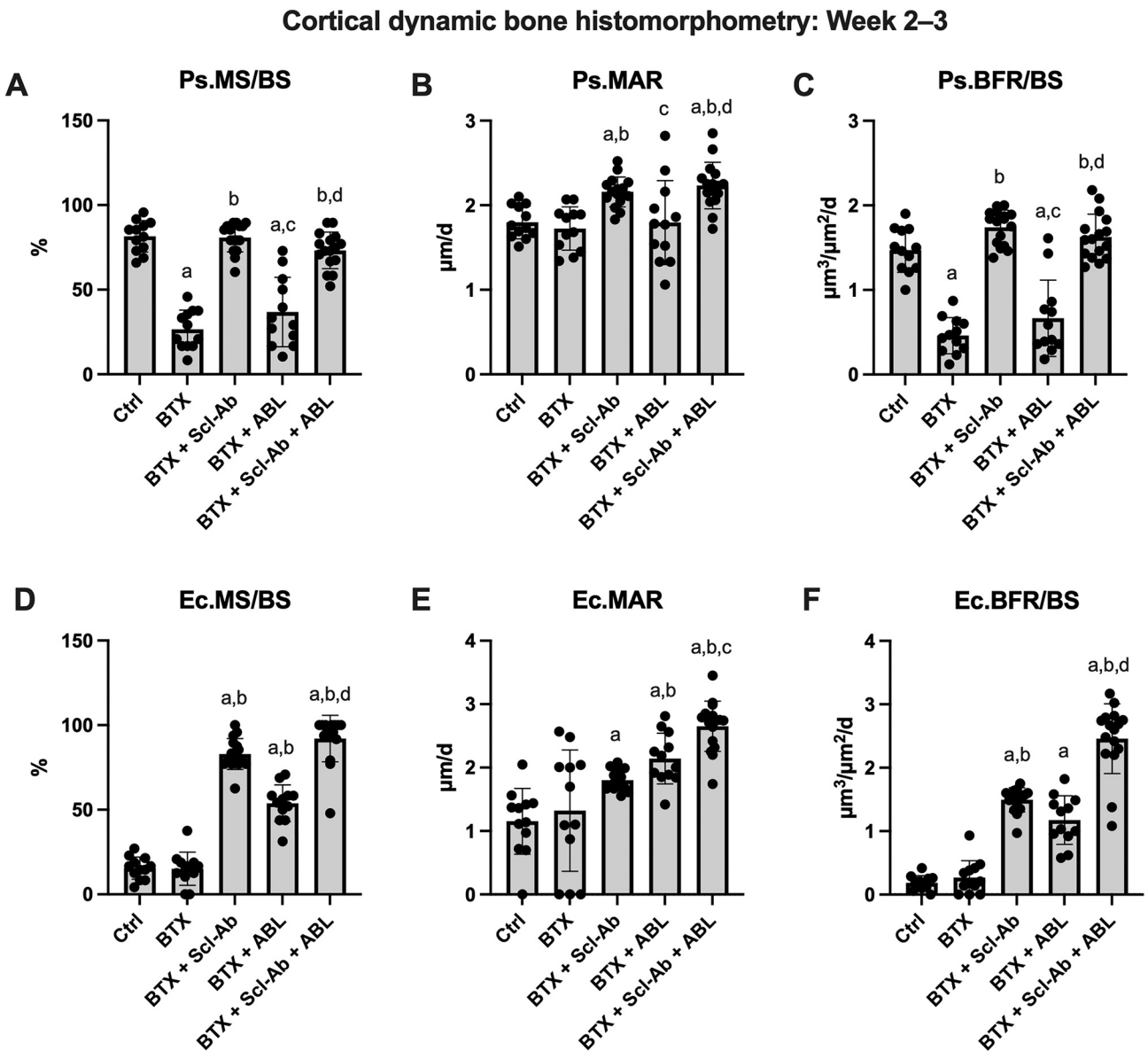

Fig. 7. A–D) Cortical dynamic bone histomorphometry at the femoral mid-diaphysis of rats subjected to hind limb disuse and treated with romosozumab (Scl-Ab) or abaloparatide (ABL) alone or in combination for four weeks. Periosteal surface (Ps), endocortical surface (Ec), mineralizing surface (MS/BS), mineral apposition rate (MAR), and bone formation rate (BFR/BS). Data are presented as mean ± SD. [a]: $p < 0.05$ vs. Ctrl. [b]: $p < 0.05$ vs. BTX. [c]: $p < 0.05$ vs. BTX + Scl-Ab. [d]: $p < 0.05$ vs. BTX + ABL.

respectively. Finally, ABL significantly increased aBMD (+7%, $p = 0.010$) compared with BTX, but not to a level significantly above that of Ctrl rats (Fig. 2).

These findings suggest that Scl-Ab combined with ABL is superior to either treatment alone in promoting increased aBMD and BMC in disuse-challenged rats. In addition, the osteoanabolic effect of Scl-Ab and ABL is additive when the treatment is combined.

3.4. µCT

3.4.1. Femoral mid-diaphysis

At the femoral mid-diaphysis, disuse significantly reduced bone area (B.Ar) (−7%, $p = 0.036$), but not cortical thickness (Ct.Th), marrow area (Ma.Ar), tissue area (T.Ar), or bone area/tissue area (BA/TA). Treatment with Scl-Ab significantly increased Ct.Th (+14%, $p < 0.001$), B.Ar (+12%, $p < 0.001$), and BA/TA (+9%, $p < 0.001$) compared with BTX, whereas treatment with ABL did not. In addition, monotherapy with Scl-Ab significantly decreased Ma.Ar (−16%, $p = 0.002$) compared with Ctrl. Scl-Ab and ABL in combination completely prevented the disuse-induced reduction in B.Ar. The increased Ct.Th (+13%, $p < 0.001$), B.Ar (+11%, $p < 0.001$), and BA/TA (+10%, $p < 0.001$) induced by treatment with Scl-Ab + ABL were significantly above that of Ctrl rats. Moreover, the increased B.Ar (+7%, $p < 0.001$ and + 16%, $p = 0.017$) was significantly above that of rats treated with Scl-Ab or ABL alone, respectively (Fig. 3).

These findings suggest the combination of Scl-Ab and ABL completely prevents mid-diaphyseal bone loss from disuse and that the treatment combination provides an additive osteoanabolic effect.

In two rats treated with Scl-Ab + ABL, a distinct and substantial amount of trabecular bone was found in the femoral diaphyseal marrow cavity. The intramedullary trabecular bone was so pronounced that it extended from the femoral neck to the distal metaphysis (Fig. 4). A trend towards increased intramedullary trabecular bone volume/tissue volume (BV/TV) was found in rats treated with Scl-Ab + ABL compared

Table 3
Dynamic bone histomorphometry at the femoral mid-diaphysis and tibial proximal metaphysis from rats subjected to hind limb disuse and treated with romosozumab (Scl-Ab) or abaloparatide (ABL) for four weeks. Periosteal surface (Ps), Endocortical surface (Ec), mineralizing surface (MS/BS), mineral apposition rate (MAR), and bone formation rate (BFR/BS). Data are presented as mean ± SD.

	Ctrl	BTX	BTX + Scl-Ab	BTX + ABL	BTX + Scl-Ab + ABL
Cortical bone: week 0–1					
Ps.MS/BS (%)	88.8 ± 9.10	53.1[a] ± 12.4	85.7[b] ± 7.09	63.7[a,c] ± 13.5	80.3[b,d] ± 10.8
Ps.MAR (μm/d)	1.90 ± 0.30	2.03 ± 0.39	2.51[a,b] ± 0.28	2.09 ± 0.37	2.79[a,b,d] ± 0.62
Ps.BFR/BS ($\mu m^3/\mu m^2$/d)	1.70 ± 0.40	1.06[a] ± 0.24	2.16[a,b] ± 0.34	1.35[c] ± 0.44	2.27[a,b,d] ± 0.67
Ec.MS/BS (%)	30.1 ± 13.1	28.8 ± 8.99	82.0[a,b] ± 12.5	44.6[c] ± 13.3	90.1[a,b,d] ± 8.66
Ec.MAR (μm/d)	1.03 ± 0.88	0.84 ± 0.90	2.03[a,b] ± 0.37	1.38[c] ± 0.58	2.74[a,b,c,d] ± 0.35
Ec.BFR/BS ($\mu m^3/\mu m^2$/d)	0.37 ± 0.42	0.25 ± 0.29	1.69[a,b] ± 0.47	0.66[b,c] ± 0.38	2.47[a,b,c,d] ± 0.38
Trabecular bone: week 0–1					
MS/BS (%)	27.9 ± 3.19	17.4[a] ± 4.25	33.7[a,b] ± 6.66	30.5[b] ± 4.45	36.9[a,b,d] ± 4.88
MAR (μm/d)	0.97 ± 0.12	0.70[a] ± 0.25	1.63[a,b] ± 0.23	1.24[a,b,c] ± 0.19	1.94[a,b,c,d] ± 0.27
BFR/BS ($\mu m^3/\mu m^2$/d)	0.27 ± 0.03	0.12[a] ± 0.05	0.56[a,b] ± 0.09	0.37[a,b,c] ± 0.06	0.71[a,b,c,d] ± 0.09

[a] $p < 0.05$ vs. Ctrl.
[b] $p < 0.05$ vs. BTX.
[c] $p < 0.05$ vs. BTX + Scl-Ab.
[d] $p < 0.05$ vs. BTX + ABL.

with BTX, although not reaching the level of significance due to substantial variations (Table 2).

The pronounced intramedullary trabecular bone formation seen in a few of the animals suggests that these rats are *"super responders"* and highly susceptible to treatment with the combination of Scl-Ab and ABL.

3.4.2. Distal femoral epiphysis

Disuse significantly reduced BV/TV (−19%, $p = 0.003$) and volumetric bone mineral density (vBMD) (−16%, $p = 0.002$) compared with ambulating Ctrl rats. No significant differences were found for trabecular thickness (Tb.Th), trabecular number (Tb.N), trabecular spacing (Tb.Sp), or connectivity density (CD) between BTX and Ctrl rats. Treatment with Scl-Ab alone significantly increased BV/TV (+59%, $p < 0.001$), Tb.Th (+65%, $p < 0.001$), tissue mineral density (TMD) (+2%, $p < 0.001$), and vBMD (48%, $p < 0.001$), while Tb.Sp (−12%, $p = 0.005$) and connectivity density (CD) (−33%, $p < 0.001$) were decreased compared with BTX rats. In addition, Scl-Ab significantly increased BV/TV (+30%, $p < 0.001$) and Tb.Th (+42%, $p < 0.001$) above that of Ctrl rats. Treatment with ABL alone significantly increased vBMD (+13%, $p = 0.032$) compared with BTX, but did not affect any other trabecular microstructural parameter assessed. Scl-Ab in combination with ABL completely prevented the disuse-induced trabecular deterioration and significantly increased bone BV/TV (+62%, $p < 0.001$), Tb.Th (+58%, $p < 0.001$), Tb.N (+32%, $p < 0.001$), TMD (+2%, $p < 0.001$), and vBMD (+48%, $p < 0.001$) above that of Ctrl rats. Moreover, Scl-Ab + ABL significantly decreased trabecular spacing (−26%, $p < 0.001$), CD (−8%, $p = 0.018$), and structure model index (SMI) (−587%, $p < 0.001$) compared with BTX rats. Finally, the combination of Scl-Ab and ABL significantly increased BV/TV (+25%, $p < 0.001$ and + 73%, $p < 0.001$) and vBMD (+19%, $p < 0.001$ and + 56%, $p < 0.001$) above that obtained with Scl-Ab or ABL alone, respectively (Fig. 5 and Table 2).

These findings suggest that the combination of Scl-Ab and ABL completely prevents the disuse-induced trabecular deterioration at the distal femoral epiphysis. In addition, the combined treatment resulted in effects on BV/TV and vBMD that were additive.

3.4.3. Distal femoral metaphysis

Disuse did not deteriorate trabecular microstructure at the distal femoral metaphysis. Treatment with Scl-Ab significantly increased Tb.Th (+57%, $p = 0.002$) and decreased Tb.N (−25%, $p < 0.001$) and CD (−57%, $p < 0.001$) compared with Ctrl rats. Aside from a significantly reduced Tb.N (−18%, $p = 0.020$) compared with Ctrl, treatment with ABL did not affect any other trabecular microstructural parameter assessed. The combination of Scl-Ab and ABL significantly increased BV/TV (+47%, $p < 0.001$), Tb.Th (+81%, $p < 0.001$), and vBMD (+33%, $p < 0.001$) and reduced CD (−53%, $p < 0.001$) compared with Ctrl. In addition, Scl-Ab + ABL increased BV/TV (+47%, $p < 0.001$ and +62%, $p < 0.001$) to a level significantly above that obtained by treatment with Scl-Ab or ABL as monotherapy, respectively (Fig. 5 and Table 2).

These findings suggest that Scl-Ab in combination with ABL is superior to either treatment alone. In addition, the effect of Scl-Ab and ABL on distal femoral metaphyseal BV/TV was additive.

3.5. Mechanical testing

Compared with Ctrl rats, disuse significantly reduced femoral neck (−29%, $p = 0.011$) and distal femoral metaphyseal bone strength (−22%, $p = 0.001$).

Monotherapy with Scl-Ab significantly increased bone strength at the mid-diaphysis (+17%, $p = 0.004$), neck (+51%, $p < 0.001$), and distal metaphysis (+27%, $p < 0.001$) compared with BTX, whereas ABL did not. Scl-Ab and ABL in combination significantly increased bone strength at all skeletal sites compared with BTX; +25% ($p < 0.001$) at the mid-diaphysis, +53% ($p < 0.001$) at the neck, and +49% ($p < 0.001$) at the distal metaphysis. Moreover, mid-diaphyseal (+14%, $p = 0.007$) and distal metaphyseal (+17%, $p = 0.007$) bone strength were significantly above that of Ctrl rats. Furthermore, the distal metaphyseal bone strength (+18%, $p = 0.002$ and +30%, $p < 0.001$) was significantly above that obtained with either Scl-Ab or ABL as monotherapy, respectively (Fig. 6).

These findings suggest treatment with Scl-Ab in combination with ABL completely prevents the disuse-induced reduction in bone strength at the distal femoral metaphysis and femoral neck and that the effects of Scl-Ab and ABL on distal femoral metaphyseal bone strength are additive.

3.6. Dynamic bone histomorphometry

3.6.1. Cortical bone

At the periosteal surface of the femoral mid-diaphysis, disuse significantly reduced mineralizing surface (MS/BS) (−40%, $p < 0.001$ and −67%, $p < 0.001$) and bone formation rate (BFR/BS) (−38%, $p = 0.006$ and −68%, $p < 0.001$) at week 0–1 and week 2–3, respectively. Scl-Ab monotherapy significantly increased MS/BS (+61%, $p < 0.001$ and +204%, $p < 0.001$), mineral apposition rate (MAR) (+24%, $p = 0.024$ and +28%, $p = 0.002$), and BFR/BS (+104%, $p < 0.001$ and +278%, $p < 0.001$) compared with BTX rats at week 0–1 and 2–3, respectively. In contrast, ABL monotherapy had no effect on the periosteal surface. Scl-Ab and ABL in combination significantly increased MS/BS (+51%, $p < 0.001$ and +176%, $p < 0.001$), MAR (+37%, $p = 0.024$ and +29%, $p < 0.001$), and BFR/BS (+114%, $p < 0.001$ and +254%, $p < 0.001$) compared with BTX at week 0–1 and 2–3, respectively (Fig. 7 and Table 3).

At the endocortical surface of the femoral mid-diaphysis, disuse had no effect on the bone remodeling indices at any time point. Scl-Ab monotherapy significantly increased MS/BS (+173%, $p < 0.001$ and +435%, $p < 0.001$), MAR (+97%, $p = 0.001$ and +57%, $p = 0.010$), and

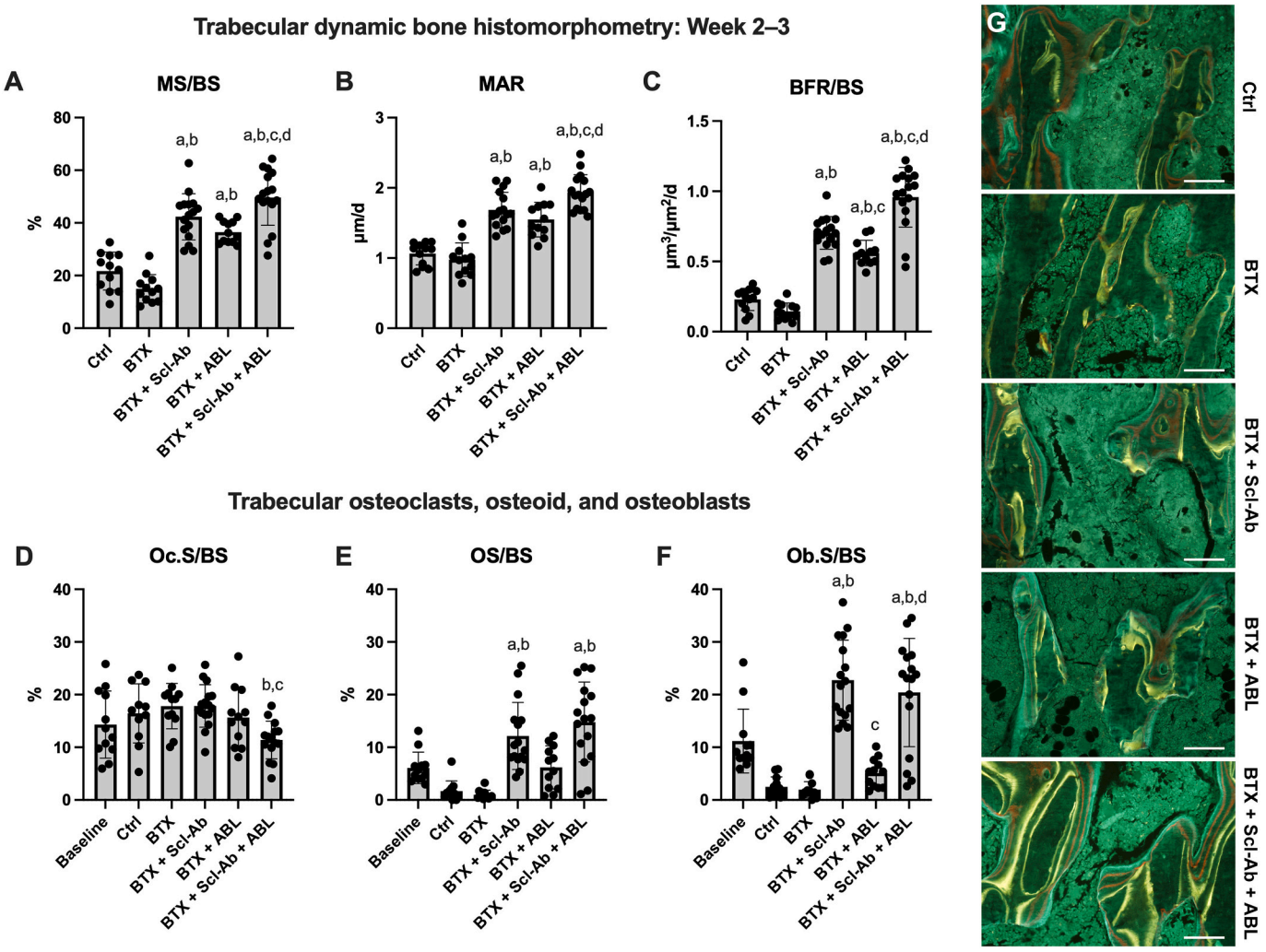

Fig. 8. Histomorphometry of proximal tibial bone of rats subjected to hindlimb disuse and treated with romosozumab (Scl-Ab) or abaloparatide (ABL) alone or in combination for four weeks. A–C) Dynamic bone histomorphometry. (D–E) Osteoclasts-covered (Oc.S/BS), osteoid-covered (OS/BS), and osteoblast-covered surfaces (Ob.S/BS). (G) Fluorochrome labels used to assess bone remodeling with dynamic bone histomorphometry (yellow: tetracycline and red: alizarin). Data are presented as mean ± SD. Bar = 100 µm. [a]: $p < 0.05$ vs. Ctrl. [b]: $p < 0.05$ vs. BTX. [c]: $p < 0.05$ vs. BTX + Scl-Ab. [d]: $p < 0.05$ vs. BTX + ABL. (For interpretation of the references to colour in this figure legend, the reader is referred to the web version of this article.)

BFR/BS (+357%, $p < 0.001$ and +728%, $p < 0.001$) compared with Ctrl at week 0–1 and 2–3, respectively. ABL monotherapy significantly increased MAR (+86%, $p < 0.001$), and BFR/BS (+550%, $p = 0.042$) at week 2–3, compared with ambulating Ctrl rats. The combination of Scl-Ab and ABL significantly increased MS/BS (+200%, $p < 0.001$ and +494%, $p < 0.001$), MAR (+166%, $p < 0.001$ and +130%, $p < 0.001$), and BFR/BS (+568%, $p < 0.001$ and +1267%, $p < 0.001$) compared with Ctrl rats at week 0–1 and 2–3, respectively. In addition, the combination treatment also increased MS/BS (+71%, $p = 0.008$) and BFR/BS (+110%, $p = 0.019$) significantly above that obtained with ABL and significantly increased MAR (+47%, $p < 0.001$) above that obtained with Scl-Ab at week 2–3 (Fig. 7 and Table 3).

These findings suggest that BTX-induced disuse mainly manifests at the periosteal surface in rats and that the effect is most pronounced early in the study. The combination of Scl-Ab and ABL substantially increased remodeling indices to a level above that obtained by either treatment alone. Moreover, the effects of the two treatments on the dynamical histomorphometric parameters on endocortical cortical bone are additive.

3.6.2. Trabecular bone

At the tibial proximal metaphysis, disuse significantly decreased MS/BS (−38%, $p < 0.001$), MAR (−28%, $p = 0.011$), and BFR/BS (−56%, $p < 0.001$) compared with Ctrl rats at week 0–1. In contrast, disuse had no significant effect at week 2–3.

Scl-Ab significantly increased MS/BS (+21%, $p = 0.018$ and +95%, $p < 0.001$), MAR (+68%, $p < 0.001$ and +59%, $p < 0.001$), and BFR/BS (+100%, $p < 0.001$ and +204%, $p < 0.001$) above that of Ctrl rats at week 0–1 and 2–3, respectively. Likewise, treatment with ABL significantly increased MAR (+28%, $p = 0.011$ and +46%, $p < 0.001$) and BFR/BS (+37%, $p = 0.001$ and +143%, $p < 0.001$) above the level of Ctrl rats at week 0–1 and 2–3, respectively. ABL also significantly increased MS/BS (+68%, $p < 0.001$) compared with Ctrl at week 2–3, but not at week 0–1. The combination of Scl-Ab and ABL significantly increased MS/BS (+32%, $p = 0.001$ and +129%, $p < 0.001$), MAR (+100%, $p < 0.001$ and +82%, $p < 0.001$), and BFR/BS (+163%, $p < 0.001$ and +317%, $p < 0.001$) compared with Ctrl at week 0–1 and 2–3, respectively. Moreover, the indices of bone remodeling were significantly higher compared with those obtained by Scl-Ab or ABL monotherapy at week 0–1 and 2–3 (Fig. 8 and Table 3).

These findings suggest the skeletal effect of disuse on bone remodeling indices is most pronounced early in the study and that the combination of Scl-Ab and ABL is superior to either treatment alone.

3.7. Osteoclasts, osteoid, and osteoblasts

At the proximal tibial metaphysis, disuse did not result in any significant differences in osteoclast-covered surfaces (Oc.S/BS), osteoid-covered surfaces (OS/BS), or osteoblast-covered surfaces (Ob.S/BS) compared with Ctrl. Only treatment with Scl-Ab and ABL in combination significantly decreased the amount of Oc.S/BS (−35%, $p = 0.005$) compared with BTX.

Treatment with Scl-Ab alone or in combination with ABL significantly increased both OS/BS (+813%, $p < 0.001$ and +720%, $p < 0.001$) and Ob.S/BS (+620%, $p < 0.001$ and +775%, $p < 0.001$) compared with Ctrl rats, respectively. In contrast, treatment with ABL alone did not affect the amount of OS/BS, Ob.S/BS, or Oc.S/BS (Fig. 8).

These findings suggest that Scl-Ab alone and in combination with ABL is effective measures to increase the amount of osteoid and osteoblast-covered surfaces in disuse-challenged rats.

4. Discussion

The purpose of the present study was to investigate whether treatment with romosozumab and abaloparatide in combination elicits an additive osteoanabolic effect in disuse osteopenic rats and whether the combination treatment is superior to either treatment alone.

As expected, BTX-injections resulted in a loss of gait ability and normal motor function accompanied by detrimental musculoskeletal effects. Hence, muscle mass, aBMD, bone strength, and bone remodeling were severely reduced by the hind limb disuse. The pervasive musculoskeletal effects of injections with BTX were largely in accordance with previous studies by us and others [24,27,31–34]. Since the impact of the disuse-induced loss of bone is substantial, pharmaceutical countermeasures must be equally powerful to prevent it.

Previous studies have demonstrated that *SOST* is heavily upregulated and circulating sclerostin levels are substantially increased in response to mechanical unloading [10–12]. Therefore, sclerostin is an obvious pharmaceutical target and has previously been investigated in rats subjected to disuse induced by spinal cord injury [14] or tail suspension [15]. The study by Zhao et al. found that eight weeks of Scl-Ab (25 mg/kg/week) treatment completely prevented disuse-induced reduction of aBMD, trabecular microstructure, and bone formation [14]. All these findings were confirmed by the present study. In addition, we found that the morphological and microstructural improvements induced by treatment with Scl-Ab also translated to substantially increased bone strength. Interestingly, the present study suggests that the pervasive and substantial disuse induced bone loss can be completely prevented by only four weeks of treatment with Scl-Ab in rats.

The skeletal effects of monotherapy with abaloparatide were less pronounced than that obtained by monotherapy with Scl-Ab. Abaloparatide attenuated the disuse-induced loss of aBMD and substantially increased endocortical and trabecular bone remodeling, but did not increase bone strength. These results mostly agree with previous findings in both intact and disuse-challenged rodents [20,24,35–37].

Ominsky et al. compared the effect of Scl-Ab and teriparatide, which is structurally and functionally similar to abaloparatide [17,24,35], and found that the effect of Scl-Ab was significantly greater than that of teriparatide on vertebral vBMD and bone formation in intact rats [30]. Similar findings in favor of Scl-Ab have also been reported in a Phase IIb clinical study, where post-menopausal women were treated with either teriparatide (20 μg daily) or Scl-Ab (210 mg monthly) for 12 months [38].

Even though teriparatide and abaloparatide are similar, have 42% amino acid sequence homology, and share the same surface receptor (PTH1R) on osteoblasts, important preclinical and clinical differences exist [17]. Teriparatide has receptor preferability towards the R^0-conformation of PTH1R, while abaloparatide has the highest affinity for the R^G-conformation [39]. When teriparatide interacts with the R^0-conformation of PTH1R, it results in a prolonged increase in intracellular cyclic adenosine monophosphate (cAMP), which contrasts with the more short-lived and rapid increase in cAMP by the interaction of abaloparatide with the R^G-conformation [24,39]. A more transient and swifter cAMP increase has been suggested to reduce mRNA expression of the pro-osteoclastogenic receptor activator of nuclear factor kappa-B ligand (RANKL) thereby reducing the calcium mobilizing potential of abaloparatide compared with that of teriparatide [40,41]. The large pivotal multi-center clinical Phase III study ACTIVE demonstrated that treatment with abaloparatide significantly decreased the risk of hypercalcemia compared with teriparatide. In addition, aBMD was significantly higher in patients treated with abaloparatide compared to that obtained with teriparatide, except at the lumbar spine [42].

To our knowledge, abaloparatide has not previously been used in combination with Scl-Ab to prevent disuse-induced bone loss or treat any other bone-related diseases, while the related teriparatide has previously been combined with Scl-Ab to promote fracture healing in rats [43]. In the present study, we found that utilizing two different cellular signaling pathways was superior to either treatment alone to counteract disuse-induced bone loss, and an additive effect was elicited. Moreover, the combination of Scl-Ab and abaloparatide even increased aBMD, cortical morphology, trabecular microstructure, bone strength, and bone remodeling indices significantly above that of normal ambulating control rats. These findings and the additive effect underline the osteoanabolic potency of Scl-Ab in combination with abaloparatide.

It is tempting to speculate on the underlying mechanism behind the additive effect found when Scl-Ab is combined with abaloparatide. As circulating sclerostin levels are increased during disuse [10–12], and the osteoanabolic effect of abaloparatide is attenuated by hind limb unloading [20], it is fair to surmise that the additive effect of Scl-Ab and abaloparatide in combination is the result of diminished sclerostin levels that provides a disuse-counterbalanced optimal environment to abaloparatide to promote bone gain. Although Scl-Ab and abaloparatide mainly exert their osteoanabolic effects through different mechanisms (e.g., PTH1R stimulation or sclerostin neutralization mediated by antibodies), there might be a partial pathway overlap [44]. Studies in mice have demonstrated that bone anabolism from treatment with teriparatide and sclerostin inhibition partially overlap, because both loss or gain of function mutations of the *SOST* gene coding for sclerostin significantly reduces teriparatide-induced bone anabolism [19,45]. Nevertheless, the outcome of the present study indicates that if a functional overlap exists it does not prevent the two bone anabolic agents from having additive effect on bone density in hind limb unloaded rats. It is important to emphasize that the pathway overlap studies were conducted with teriparatide and in mice. Future studies are warranted to elucidate whether such pathway overlaps with sclerostin inhibition also occurs with abaloparatide treatment and are not limited to mice only.

Surprisingly, a few of the rats treated with Scl-Ab and abaloparatide in combination developed pronounced and widespread trabecular bone in the femoral diaphyseal marrow space (Fig. 3). Their skeletal phenotype indicates that these rats were *"super responders"* to the Scl-Ab and abaloparatide co-treatment. Pharmaceutical *"super responders"* is not a well-described phenomenon in bone research, but has previously been reported in relation to monoclonal antibody therapy for psoriasis or asthma [46,47]. *"Super responders"* might be a rare phenomenon in bone research, which is underlined by the few rats that exhibited the pronounced phenotype and by no study was found by a literature search in PubMed using the keywords "super responder" and "bone". However, it is important to recognize that individual differences in treatment susceptibility exist and that such differences might be important to monitor in order to optimize treatment efficacy and dose when using Scl-Ab and abaloparatide in combination.

The present study has some limitations. The dose of Scl-Ab and abaloparatide was selected in order to maximize bone gain and are different from those used in a clinical setting. The twice weekly dose of Scl-Ab 25 mg/kg was based on a previous tail suspension study in rats

[15]. By comparison, patients treated with Scl-Ab (romosozumab) are recommended a monthly dose of 210 mg [48]. Furthermore, the Scl-Ab used in the present study was the commercially available romosozumab, which is a humanized form of anti-sclerostin. Although the efficacy of Scl-Ab was promising, both alone and in combination with abaloparatide, ADA might have attenuated the pharmacological response [30]. ADA were not measured because all animals treated with Scl-Ab responded as expected. Others have previously used romosozumab in rats and demonstrated ADA are present in approximately 25% of the animals after 4 weeks of treatment (personal communication with Dr. Rogely Waite Boyce, Amgen Research) [30]. Another limitation is that the dose of abaloparatide (80 μg/kg/day) was relatively high compared to that used in a clinical setting (80 μg/day), but this dose was based on a previous study of BTX-immobilized rats [24]. The dose of Scl-Ab (25 mg/kg twice weekly) was based on a previous tail suspension study in rats using the same dose and demonstrating Scl-Ab prevents disuse-induced skeletal deterioration [15]. In a clinical setting, Scl-Ab is administered at a dose of 210 mg/month. Although it is difficult to directly compare doses used in laboratory animals to those used in a clinical setting, human equivalent doses (HEDs) can be estimated, which is adjusted for the differences in surface area and metabolic rate between rodents and humans [49]. HEDs for abaloparatide and Scl-Ab used in the present study are 13 μg/kg/day and 4 mg/kg twice weekly, respectively.

In conclusion, treatment with Scl-Ab alone and in combination with abaloparatide prevented disuse-induced skeletal deterioration. Moreover, the combination of Scl-Ab and abaloparatide was superior to either treatment as monotherapy. The effect of the pharmaceuticals on aBMD, cortical morphology, trabecular microstructure, bone strength, and bone formation was additive. Consequently, the combination of Scl-Ab and abaloparatide appear to be a well-suited alternative for the treatment of very severe osteoporosis, where a maximized bone gain is warranted.

CRediT authorship contribution statement

Mikkel Bo Brent: Conceptualization; resources; data curation; formal analysis; funding acquisition; validation; investigation; visualization; methodology; writing - original draft; project administration; writing - review and editing. Jesper Skovhus Thomsen: Conceptualization; resources; formal analysis; supervision; investigation; methodology; writing - review and editing. Annemarie Brüel: Conceptualization; resources; formal analysis; supervision; investigation; methodology; writing - review and editing.

Data availability statement

The data that support the findings of this study are available from the corresponding author upon reasonable request.

Declaration of competing interest

The authors declare no competing interests.

Acknowledgements

The authors are thankful for the excellent technical assistance of Jytte Utoft. We thank Visiopharm for the contribution to the stereology software system. The VELUX Foundation donated the μCT system. The study was kindly supported by Health Aarhus University and The A.P. Møller Foundation for the Advancement of Medical Science.

References

[1] J.E. Compston, M.R. McClung, W.D. Leslie, Osteoporosis, Lancet 393 (2019) 364–376, https://doi.org/10.1016/S0140-6736(18)32112-3.
[2] J.A. Kanis, E.V. McCloskey, Risk factors in osteoporosis, Maturitas 30 (1998) 229–233, https://doi.org/10.1016/S0378-5122(98)00090-5.
[3] P.D. Ross, Osteoporosis: frequency, consequences, and risk factors, Arch. Intern. Med. 156 (1996) 1399–1411, https://doi.org/10.1001/ARCHINTE.1996.00440120051005.
[4] M.B. Brent, A. Brüel, J.S. Thomsen, A systematic review of animal models of disuse-induced bone loss, Calcif. Tissue Int. 108 (2021) 561–575, https://doi.org/10.1007/s00223-020-00799-9.
[5] N. Allison, B. Brooks, Bone atrophy. An experimental and clinical study of the changes in bone which result from non−use. SurgeryGynecol. Obstet. 33 (1921) 250–260.
[6] H. Nasse, Ueber den Einfluss der Nervendurchschneidung auf die Ernährung, insbesondere auf die Form und die Zusammensetzung der Knochen, in: Arch. Für Die Gesamte Physiol. Des Menschen Und Der Tiere 23, 1880, pp. 361–405.
[7] R. Baron, M. Kneissel, WNT signaling in bone homeostasis and disease: from human mutations to treatments, Nat. Med. 19 (2013) 179–192, https://doi.org/10.1038/nm.3074.
[8] R. Baron, G. Rawadi, Targeting the Wnt/β-catenin pathway to regulate bone formation in the adult skeleton, Endocrinology 148 (2007) 2635–2643, https://doi.org/10.1210/en.2007-0270.
[9] X. Li, Y. Zhang, H. Kang, W. Liu, P. Liu, J. Zhang, S.E. Harris, D. Wu, Sclerostin binds to LRP5/6 and antagonizes canonical Wnt signaling, J. Biol. Chem. 280 (2005) 19883–19887, https://doi.org/10.1074/jbc.M413274200.
[10] C. Lin, X. Jiang, Z. Dai, X. Guo, T. Weng, J. Wang, Y. Li, G. Feng, X. Gao, L. He, Sclerostin mediates bone response to mechanical unloading through antagonizing Wnt/β-catenin signaling, J. Bone Miner. Res. 24 (2009) 1651–1661, https://doi.org/10.1359/jbmr.090411.
[11] A. Gaudio, P. Pennisi, C. Bratengeier, V. Torrisi, B. Lindner, R.A. Mangiafico, I. Pulvirenti, G. Hawa, G. Tringali, C.E. Fiore, Increased sclerostin serum levels associated with bone formation and resorption markers in patients with immobilization-induced bone loss, J. Clin. Endocrinol. Metab. 95 (2010) 2248–2253, https://doi.org/10.1210/jc.2010-0067.
[12] J.M. Spatz, M.N. Wein, J.H. Gooi, Y. Qu, J.L. Garr, S. Liu, K.J. Barry, Y. Uda, F. Lai, C. Dedic, M. Balcells-Camps, H.M. Kronenberg, P. Babij, P.D. Pajevic, The wnt inhibitor sclerostin is up-regulated by mechanical unloading in osteocytes in vitro, J. Biol. Chem. 290 (2015) 16744–16758, https://doi.org/10.1074/jbc.M114.628313.
[13] A.G. Robling, P.J. Niziolek, L.A. Baldridge, K.W. Condon, M.R. Allen, I. Alam, S. M. Mantila, J. Gluhak-Heinrich, T.M. Bellido, S.E. Harris, C.H. Turner, Mechanical stimulation of bone in vivo reduces osteocyte expression of Sost/sclerostin, J. Biol. Chem. 283 (2008) 5866–5875, https://doi.org/10.1074/jbc.M705092200.
[14] W. Zhao, X. Li, Y. Peng, Y. Qin, J. Pan, J. Li, A. Xu, M.S. Ominsky, C. Cardozo, J. Q. Feng, H.Z. Ke, W.A. Bauman, W. Qin, Sclerostin antibody reverses the severe sublesional bone loss in rats after chronic spinal cord injury, Calcif. Tissue Int. 103 (2018) 443–454, https://doi.org/10.1007/s00223-018-0439-8.
[15] X.Y. Tian, W.S.S. Jee, X. Li, C. Paszty, H.Z. Ke, Sclerostin antibody increases bone mass by stimulating bone formation and inhibiting bone resorption in a hindlimb-immobilization rat model, Bone 48 (2011) 197–201, https://doi.org/10.1016/j.bone.2010.09.009.
[16] D. Zhang, M. Hu, T. Chu, L. Lin, J. Wang, X. Li, H.Z. Ke, Y.X. Qin, Sclerostin antibody prevented progressive bone loss in combined ovariectomized and concurrent functional disuse, Bone 87 (2016) 161–168, https://doi.org/10.1016/j.bone.2016.02.005.
[17] M.B. Brent, Abaloparatide: a review of preclinical and clinical studies, Eur. J. Pharmacol. 909 (2021), 174409, https://doi.org/10.1016/j.ejphar.2021.174409.
[18] E. Quattrocchi, H. Kourlas, Teriparatide: a review, Clin. Ther. 26 (2004) 841–854, https://doi.org/10.1016/S0149-2918(04)90128-2.
[19] I. Kramer, G.G. Loots, A. Studer, H. Keller, M. Kneissel, Parathyroid hormone (PTH)-induced bone gain is blunted in SOST overexpressing and deficient mice, J. Bone Miner. Res. 25 (2010) 178–189, https://doi.org/10.1359/jbmr.090730.
[20] D.A. Teguh, J.L. Nustad, A.E. Craven, D.J. Brooks, H. Arlt, D. Hu, R. Baron, B. Lanske, M.L. Bouxsein, Abaloparatide treatment increases bone formation, bone density and bone strength without increasing bone resorption in a rat model of hindlimb unloading, Bone 144 (2021), https://doi.org/10.1016/j.bone.2020.115801.
[21] R.T. Turner, S. Lotinun, T.E. Hefferan, E. Morey-Holton, Disuse in adult male rats attenuates the bone anabolic response to a therapeutic dose of parathyroid hormone, J. Appl. Physiol. 101 (2006) 881–886, https://doi.org/10.1152/japplphysiol.01622.2005.
[22] D. Chappard, A. Chennebault, M. Moreau, E. Legrand, M. Audran, M.F. Basle, Texture analysis of X-ray radiographs is a more reliable descriptor of bone loss than mineral content in a rat model of localized disuse induced by the clostridium botulinum toxin, Bone 28 (2001) 72–79.
[23] M.B. Brent, A. Lodberg, J.S. Thomsen, A. Brüel, Rodent model of disuse-induced bone loss by hind limb injection with botulinum toxin a, MethodsX. 7 (2020), 101079, https://doi.org/10.1016/j.mex.2020.101079.
[24] M.B. Brent, J.S. Thomsen, A. Brüel, The efficacy of PTH and abaloparatide to counteract immobilization-induced osteopenia is in general similar, Front. Endocrinol. (Lausanne) 11 (2020) 808, https://doi.org/10.3389/fendo.2020.588773.
[25] S.E. Warner, D.A. Sanford, B.A. Becker, S.D. Bain, S. Srinivasan, T.S. Gross, Botox induced muscle paralysis rapidly degrades bone, Bone 38 (2006) 257–264, https://doi.org/10.1016/j.bone.2005.08.009.
[26] M.L. Bouxsein, S.K. Boyd, B.A. Christiansen, R.E. Guldberg, K.J. Jepsen, R. Müller, Guidelines for assessment of bone microstructure in rodents using micro-computed tomography, J. Bone Miner. Res. 25 (2010) 1468–1486, https://doi.org/10.1002/jbmr.141.

[27] M.B. Brent, A. Brüel, J.S. Thomsen, PTH (1–34) and growth hormone in prevention of disuse osteopenia and sarcopenia in rats, Bone 110 (2018) 244–253, https://doi.org/10.1016/j.bone.2018.02.017.
[28] D.W. Dempster, J.E. Compston, M.K. Drezner, F.H. Glorieux, J.A. Kanis, H. Malluche, P.J. Meunier, S.M. Ott, R.R. Recker, A.M. Parfitt, Standardized nomenclature, symbols, and units for bone histomorphometry: A 2012 update of the report of the ASBMR Histomorphometry Nomenclature Committee, J. Bone Miner. Res. 28 (2013) 2–17, https://doi.org/10.1002/jbmr.1805.
[29] A. Brüel, J.B. Vegger, A.C. Raffalt, J.E.T. Andersen, J.S. Thomsen, PTH (1–34), but not strontium ranelate counteract loss of trabecular thickness and bone strength in disuse osteopenic rats, Bone 53 (2013) 51–58, https://doi.org/10.1016/j.bone.2012.11.037.
[30] M.S. Ominsky, D.L. Brown, G. Van, D. Cordover, E. Pacheco, E. Frazier, L. Cherepow, M. Higgins-Garn, J.I. Aguirre, T.J. Wronski, M. Stolina, L. Zhou, I. Pyrah, R.W. Boyce, Differential temporal effects of sclerostin antibody and parathyroid hormone on cancellous and cortical bone and quantitative differences in effects on the osteoblast lineage in young intact rats, Bone 81 (2015) 380–391, https://doi.org/10.1016/j.bone.2015.08.007.
[31] T.G. Sørensen, M.B. Brent, J.S. Thomsen, A. Brüel, Disuse-induced loss of bone mineral density and bone strength is attenuated by post-lactational bone gain in NMRI mice, Bone 131 (2020), 115183, https://doi.org/10.1016/j.bone.2019.115183.
[32] M.B. Brent, A. Lodberg, F.D. Bromer, B.C.J. van der Eerden, M. Eijken, A. Brüel, J. S. Thomsen, Activin type IIA decoy receptor and intermittent parathyroid hormone in combination overturns the bone loss in disuse-osteopenic mice, Bone 142 (2021), 115692, https://doi.org/10.1016/j.bone.2020.115692.
[33] F.D. Bromer, M.B. Brent, M. Pedersen, J.S. Thomsen, A. Brüel, C.B. Foldager, The effect of normobaric intermittent hypoxia therapy on bone in normal and disuse osteopenic mice, High Alt. Med. Biol. 22 (2021) 225–234, https://doi.org/10.1089/ham.2020.0164.
[34] M.J. Tang, H.K. Graham, K.E. Davidson, Botulinum toxin a and osteosarcopenia in experimental animals: a scoping review, Toxins (Basel) 13 (2021) 213, https://doi.org/10.3390/toxins13030213.
[35] M.B. Brent, F.E. Stoltenborg, A. Brüel, J.S. Thomsen, Teriparatide and abaloparatide have a similar effect on bone in mice, Front. Endocrinol. (Lausanne) 12 (2021) 328, https://doi.org/10.3389/fendo.2021.628994.
[36] A. Makino, T. Hasegawa, H. Takagi, Y. Takahashi, N. Hase, N. Amizuka, Frequent administration of abaloparatide shows greater gains in bone anabolic window and bone mineral density in mice: a comparison with teriparatide, Bone 142 (2020), 115651, https://doi.org/10.1016/j.bone.2020.115651.
[37] C. Le Henaff, F. Ricarte, B. Finnie, Z. He, J. Johnson, J. Warshaw, V. Kolupaeva, N. C. Partridge, Abaloparatide at the same dose has the same effects on bone as PTH (1–34) in mice, J. Bone Miner. Res. 35 (2020) 714–724, https://doi.org/10.1002/jbmr.3930.
[38] M.R. McClung, A. Grauer, S. Boonen, M.A. Bolognese, J.P. Brown, A. Diez-Perez, B. L. Langdahl, J.-Y. Reginster, J.R. Zanchetta, S.M. Wasserman, L. Katz, J. Maddox, Y.-C. Yang, C. Libanati, H.G. Bone, Romosozumab in postmenopausal women with low bone mineral density, N. Engl. J. Med. 370 (2014) 412–420, https://doi.org/10.1056/NEJMoa1305224.
[39] G. Hattersley, T. Dean, B.A. Corbin, H. Bahar, T.J. Gardella, Binding selectivity of abaloparatide for PTH-type-1-receptor conformations and effects on downstream signaling, Endocrinology 157 (2016) 141–149, https://doi.org/10.1210/en.2015-1726.
[40] F.R. Ricarte, C. Le Henaff, V.G. Kolupaeva, T.J. Gardella, N.C. Partridge, Parathyroid hormone(1–34) and its analogs differentially modulate osteoblastic rankl expression via PKA/SIK2/SIK3 and PP1/PP2A–CRTC3 signaling, J. Biol. Chem. 293 (2018) 20200–20213, https://doi.org/10.1074/jbc.RA118.004751.
[41] S.H. Tella, A. Kommalapati, R. Correa, Profile of abaloparatide and its potential in the treatment of postmenopausal osteoporosis, Cureus 9 (2017), https://doi.org/10.7759/cureus.1300.
[42] P.D. Miller, G. Hattersley, B.J. Riis, G.C. Williams, E. Lau, L.A. Russo, P. Alexandersen, C.A.F. Zerbini, M.Y. Hu, A.G. Harris, L.A. Fitzpatrick, F. Cosman, C. Christiansen, Effect of abaloparatide vs placebo on new vertebral fractures in postmenopausal women with osteoporosis a randomized clinical trial, J. Am. Med. Assoc. 316 (2016) 722–733, https://doi.org/10.1001/jama.2016.11136.
[43] J. Lin, J. Wu, S. Sun, K. Chen, H. Wu, R. Lin, C. Zhou, J. Kong, K. Zhou, X. Shui, Combined antisclerostin antibody and parathyroid hormone (1–34) synergistically enhance the healing of bone defects in ovariectomized rats, Z. Gerontol. Geriatr. 53 (2020) 163–170, https://doi.org/10.1007/s00391-019-01685-2.
[44] H. Keller, M. Kneissel, SOST is a target gene for PTH in bone, Bone 37 (2005) 148–158, https://doi.org/10.1016/j.bone.2005.03.018.
[45] I. Kramer, H. Keller, O. Leupin, M. Kneissel, Does osteocytic SOST suppression mediate PTH bone anabolism? Trends Endocrinol. Metab. 21 (2010) 237–244, https://doi.org/10.1016/j.tem.2009.12.002.
[46] R. Ruiz-Villaverde, L. Rodriguez-Fernandez-Freire, J.C. Armario-Hita, A. Pérez-Gil, M. Galán-Gutiérrez, Super responders to guselkumab treatment in moderate-to-severe psoriasis: a real clinical practice pilot series, Int. J. Dermatol. (2021), https://doi.org/10.1111/ijd.15784.
[47] C. Rodríguez-García, M. Blanco-Aparicio, J.J. Nieto-Fontarigo, N. Blanco-Cid, C. Gonzalez-Fernandez, M. Mosteiro-Añon, U. Calvo-Alvarez, L. Perez-De-Llano, M. D. Corbacho-Abelaira, T. Lourido-Cebreiro, L.M. Dominguez-Juncal, C. Crespo-Diz, R. Dacal-Quintas, A. Pallares-Sanmartin, D. Dacal-Rivas, F.J. Gonzalez-Barcala, Efficacy of mepolizumab in usual clinical practice and characteristics of responders: mepolizumab in usual clinical practice, Respir. Med. 187 (2021), https://doi.org/10.1016/j.rmed.2021.106595.
[48] F. Cosman, D.B. Crittenden, J.D. Adachi, N. Binkley, E. Czerwinski, S. Ferrari, L. C. Hofbauer, E. Lau, E.M. Lewiecki, A. Miyauchi, C.A.F. Zerbini, C.E. Milmont, L. Chen, J. Maddox, P.D. Meisner, C. Libanati, A. Grauer, Romosozumab treatment in postmenopausal women with osteoporosis, N. Engl. J. Med. 375 (2016) 1532–1543, https://doi.org/10.1056/nejmoa1607948.
[49] A. Nair, S. Jacob, A simple practice guide for dose conversion between animals and human, J. Basic Clin. Pharm. 7 (2016) 27, https://doi.org/10.4103/0976-0105.177703.